

Mechanical Compliance Control System for A Pneumatic Robot Arm

Kouichi Watanabe¹, Hisashi Nagayasu¹, Naoki Kawakami¹ and Susumu Tachi¹,

¹Department of Information Physics and Computing, The University of Tokyo, Tokyo, Japan
(Tel : +81-3-5841-6917;

E-mail: {Kouichi_Watanabe, Hisashi_Nagayasu}@ipc.i.u-tokyo.ac.jp
{kawakami, tachi}@star.t.u-tokyo.ac.jp)

Abstract: The design and control of robots from the perspective of human safety is desired. We propose a Mechanical Compliance Control System as a new pneumatic arm control system. However, safety against collisions with obstacles in an unpredictable environment is difficult to insure in previous system. The main feature of the proposed system is that the two desired pressure values are calculated by using two other desired values, the end compliance of the arm and the end position and posture of the arm.

Keywords: Pneumatic actuator, Humanoid robot arm, Compliance control

1. INTRODUCTION

Many human coexistence-type robots are being developed in order to achieve a human-robot coexistence society. In particular, robots that interact with humans actively, such as AIBO or ASIMO, are emerging. Therefore, the design and control of robots from the perspective of human safety is desired.

As a control system for robots actuated by motors for the purpose of safety, an impedance control system had been proposed [1]. However, safety against collisions with obstacles in an unpredictable environment is difficult to insure in this system. In addition, the size and weight of robots increases because the ratio of the output power to the weight of the motor is small. Therefore, the safety of this system is inadequate. We propose a "Mechanical Compliance Control System" as a new pneumatic arm control system to solve the above-mentioned problems. Consequently, we have focused on a pneumatic actuator as a robot actuator.

The pneumatic actuator's safety is intrinsic because of it being passive compliant due to the compressibility of air and being explosion proof, and possessing high back-drivability. In addition, this actuator can exert enough driving power despite being lightweight and having a small size because the ratio of its output power to its weight is large. An avoidance motion when a collision occurs is an important function for human-robot interaction. Therefore, the pneumatic actuator having these properties is available for human coexistence-type robots.

Various types of pneumatic actuators such as a pneumatic rubber artificial muscle and a pneumatic cylinder have been developed, and their features and characteristics are different in several respects. (Fig. 1 shows an example of the latter). The pneumatic actuators have started gaining attention as robot actuators. We focused on the robot arm using a pneumatic cylinder because of its high power, high stiffness, small size, simple configuration, and ease of modeling.

There exist many researches regarding the position control of a robot arm using the pneumatic actuators. On the other hand, there exists little research for compliance

control using aggressively properties of air pressures. In the field of industrial robots, the compliance control of a robot arm is either passive control-type or feedback control-type. On the other hand, in human life space, the compliance control should both be active control-type and real-time control-type. In general, a pneumatic cylinder servo system can achieve the desired compliance easily because it can change its compliance just by changing the pressure. Thus, we have considered controlling the compliance of a humanoid arm using a pneumatic cylinder servo system.

In this paper, we present an overview of the system and explain the control section of the system. The pneumatic arm used in this paper is virtually identical to mentioned in [2] in terms of configuration and performance. However, control law and system as satisfying desired position and posture and desired compliance is not proposed in [2]. Model-based control should be used in proposed system to control the compliance before collision with obstacles. Therefore, we propose not only Mechanical Compliance Control System and also the modeling of a pneumatic arm for real.



Fig. 1 Robot arm using pneumatic cylinder.

2. MECHANICAL COMPLIANCE CONTROL SYSTEM

2.1 Overview of System

Our proposed control system can determine the adequate inner pressures of pneumatic chambers when the desired end compliance and the desired end position and posture of the arm have been specified. Fig. illustrates a system diagram of the proposed system. As shown in Fig. , there are two main control flows –compliance control flow and position control flow– in this system. The main feature of this system is that the two desired pressure values can be calculated by using the two desired values –the end compliance and end position and posture of the arm. Although we should consider seven degrees of freedom under normal condition, we consider only one degree of freedom because extension of degrees of freedom is easy.

Note that we define a measure of compliance as reciprocal of spring stiffness. The compliance C is represented by following equation.

$$C \triangleq \frac{dx}{dF} \left(C \triangleq \frac{d\theta}{dM} \right) \quad (1)$$

where dF is external force (dM is moment) and dx is displacement caused by dF ($d\theta$ is each joint displacement).

2.2 Definition of Parameters

In this subsection, we define any parameters using following sections.

(x_*, y_*) is Cartesian coordinates.

l_* is rod length.

P_1, P_2 are pressures.

A_1, A_r are cross section of piston and rod.

θ, ϕ, η are angles.

τ is torque.

F is inner force of pneumatic cylinder.

r is screw radius.

C_{jnt}, C_{cyl} are compliance of each joints and each pneumatic cylinders, respectively.

2.3 Position Control Flow

In the position control flow, the desired joint angles are obtained by inverse kinematics from the desired end position and posture of the arm. The desired joint angles are then translated to the desired cylinder position by using a transform function (T_p). They are used as the input data of the position control block, and a relational expression ($f^* = 0$) of the pneumatic chamber pressure is generated. In Fig. 2, while the position control block represents an I-PD control system, any position control law such as an adaptive control law can be applied to this block if only it generates a relational expression of the pneumatic chamber pressures.

$$\begin{aligned} f^*(P_1, P_2) &= F - F^* \\ &= A_1 P_1 - A_2 P_2 - A_r P_A - F^* = 0, \end{aligned} \quad (2)$$

$$\begin{aligned} F^* &\triangleq -K_p x + K_I \int_{\tau=0}^t (x^* - x) d\tau \\ &\quad - K_D \frac{dx}{dt} \end{aligned} \quad (3)$$

where x is end position of piston with direction to piston rod from lower limit of cylinder. Fig. 3 shows the relation of each parameters of the pneumatic cylinder.

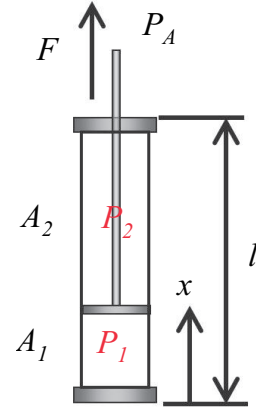


Fig. 3 Pneumatic cylinder model. .

2.4 Compliance Control Flow

In the compliance control flow, Direct Compliance Control (DCC) [3] converts the desired end compliance of the arm to the desired joint compliance. The desired joint compliance is then translated to the desired cylinder compliance by using a transform function. The relational expression of the pneumatic chamber pressures are obtained from the desired cylinder compliance using an appropriate model-based control law (G).

2.5 Proposed Cylinder Compliance Control

Next, we present a relational equation for determining the desired pneumatic chamber pressures in the compliance control flow. It is desirable to be able to control the compliance before collision with obstacles for this arm. Therefore, it should be used a model-based control, and modeling of the pneumatic arm is needed. As mentioned in Section 1, the configuration of pneumatic arm is simple and modeling is easy. Then, we control cylinder compliance by using the model-based control law.

NORITSUGU et al. have proposed the relational equation of cylinder compliance as follows [4].

$$f^*(P_1, P_2) = \kappa C_{cyl}^* \left(A_1 \frac{P_1}{x} + A_2 \frac{P_2}{l-x} \right) + 1 = 0 \quad (4)$$

where l is cylinder length and κ is ratio of specific heat.

The desired pneumatic chamber pressures are determined from a solution of the simultaneous equations () and () obtained in Section 2.2 and 2.4, respectively.

By using this control method the compliance can be changed in real-time before a collision with obstacles occurs. Furthermore, the proposed system can be applied to the pneumatic robot arms if only the general information (position, posture, and pressures) of the robot arms can be acquired. Consequently, it is considered that the application of the proposed system to a real system is possible.

3. MODELING OF PNEUMATIC ARM

3.1 Overview of Pneumatic Arm

In this Section, we use the pneumatic arm actually constructed and modeling of this arm and develop the expression for transform function.

We use the pneumatic arm shown in Fig. 1. Joint mechanism of the robot arm using pneumatic actuators is generally complication as compared with a robot arm using DC motors. However, in all of pneumatic actuators the pneumatic cylinder has simple mechanism compared with other pneumatic actuators. Therefore, modeling of it can obtain geometrically. In following sections, we construct the model of pneumatic arm and propose that the result of modeling is obtained relatively easy. This mechanism is one of examples, other pneumatic cylinder arm will be obtained geometrically as well.

3.2 Frame arrangement and DH Parameters

Joint motion ranges of pneumatic arm and arrangement of link frames x_i - y_i - z_i are shown in Fig. 4. We use DH parameters notation as the manner of frame arrangement. In this notation, we arrange the origin of base frame X - Y - Z on the shoulder. Table 1 shows DH parameters.

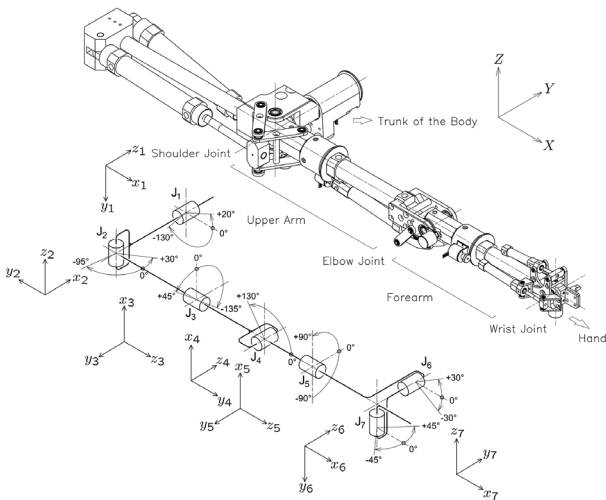


Fig. 4 Range of movement and frame arrangement (right arm).

Table 1 Link parameter of Denavit-Hartenberg notation(right arm)

frame[$\{i\}$]	a_{i-1} [m]	d_i [m]	α_{i-1} [rad]	θ_i [rad]
1	0	0	$-\frac{\pi}{2}$	θ_1
2	0	0	$\frac{\pi}{2}$	$\theta_2 + \frac{\pi}{2}$
3	0	L_{upper}	$\frac{\pi}{2}$	$\theta_3 + \frac{\pi}{2}$
4	0	0	$\frac{\pi}{2}$	θ_4
5	0	L_{fore}	$-\frac{\pi}{2}$	θ_5
6	0	0	$\frac{\pi}{2}$	$\theta_6 + \frac{\pi}{2}$
7	0	0	$\frac{\pi}{2}$	θ_7
end effector	$L_{a\text{end}}$	$L_{d\text{end}}$	$A_{\alpha\text{end}}$	$A_{\theta\text{end}}$

3.3 Joint Classification and Modeling

We divide the seven joints of the pneumatic arm into three types of mechanisms; 3 link + 4 link mechanism, screw mechanism and 3 link mechanism. Joint 1, 2, and 4 are classified into 3 link + 4 link mechanism, Joint 3 and 5 are screw mechanism and Joint 6 and 7 are 3 link mechanism. In following subsections, we present the modeling of these link mechanisms and transform functions. Transform functions consist of four functions; transform from joint compliance to cylinder compliance T_c , from joint angle to cylinder position T_p , from joint angular velocity to cylinder velocity T_v and from joint torque to cylinder pressure T_f .

3.3.1 3 link + 4 link mechanism

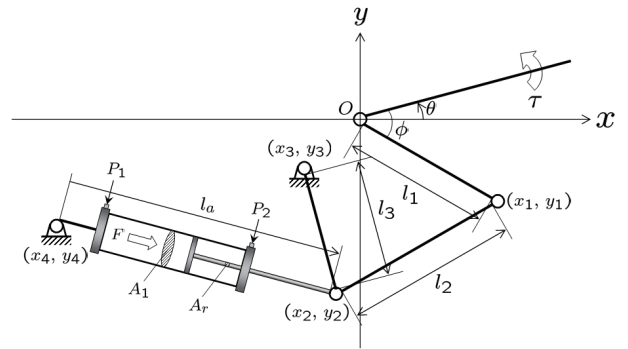


Fig. 5 .

From Fig. 5, next equations are obtained geometrically.

$$x_1 = l_1 \cos(\theta + \phi), \quad (20)$$

$$y_1 = l_1 \sin(\theta + \phi), \quad (21)$$

$$l_a = \sqrt{(x_2 - x_4)^2 + (y_2 - y_4)^2} \quad (22)$$

From these equation, T_p is

$$l_a = \sqrt{\{TMP1\}^2 + \{TMP2\}^2} \quad (23)$$

$$\triangleq T_p(\theta), \quad (24)$$

where TMP1 and TMP2 are

$$\begin{aligned} TMP1 &= x_1 + q_2(x_3 - x_1) - q_3(y_3 - y_1) - x_4, \\ TMP2 &= y_1 + q_2(y_3 - y_1) + q_3(x_3 - x_1) - y_4 \\ q_2 &\triangleq \frac{l_2^2 - l_3^2 + q_1}{2q_1}, \\ q_3 &\triangleq \sqrt{\frac{-(l_2^2 - l_3^2)^2 + 2(l_2^2 + l_3^2)q_1 - q_1^2}{4q_1^2}} \end{aligned} \quad (25)$$

$$(26)$$

From derivation of T_p, T_v is

$$\begin{aligned} \frac{dl_a}{dt} &= \frac{1}{2\sqrt{(x_2 - x_4)^2 + (y_2 - y_4)^2}} \\ &\left\{ 2(x_2 - x_4)\frac{dx_2}{dt} + 2(y_2 - y_4)\frac{dy_2}{dt} \right\} \\ &\triangleq T_v \left(\theta, \frac{d\theta}{dt} \right) \end{aligned} \quad (27)$$

$$(28)$$

From equilibrium of force and torque, T_f is

$$\begin{aligned} T_f(P_1, P_2, \tau, \theta) &\triangleq A_1 P_1 - A_2 P_2 - A_r P_A - \frac{1}{R(\theta)} \tau \\ &= 0 \end{aligned} \quad (29)$$

In addition, T_c is

$$\begin{aligned} C_{cyl} &= \frac{R(\theta)l_\theta(\theta)}{\frac{1}{C_{jnt}} - \frac{dR(\theta)}{d\theta} (A_1 P_1 - A_2 P_2 - A_r P_A)} \\ &\triangleq T_C(\theta, P_1, P_2, C_{jnt}) \end{aligned} \quad (30)$$

3.3.2 Screw mechanism

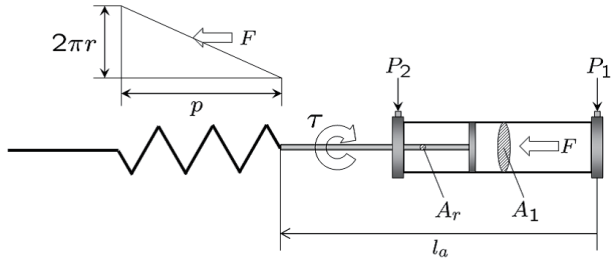


Fig. 6 .

From Fig. 6, next equations are obtained geometrically.

$$\frac{p}{2\pi r} \frac{dl_a}{dt} = r \frac{d\theta}{dt} \quad (31)$$

Thus, T_v is

$$\frac{dl_a}{dt} = \frac{2\pi r^2}{p} \frac{d\theta}{dt} \triangleq T_v \left(\frac{d\theta}{dt} \right) \quad (32)$$

Therefore, T_p is

$$l_a = \frac{2\pi r^2}{p} \theta + l_{a_o} \quad (33)$$

$$\triangleq T_p(\theta) \quad (34)$$

where l_{a_o} is l_a in condition of $\theta = 0$.

Also, from Fig. 6, T_f is

$$\begin{aligned} T_f(P_1, P_2, \tau) &\triangleq A_1 P_1 - A_2 P_2 - A_r P_A - \frac{1}{R} \tau \\ &= 0 \end{aligned} \quad (35)$$

In addition, from the force relation in the cylinder, T_c is

$$\frac{1}{C_{jnt}} = \frac{d\tau}{d\theta} = R \frac{dF}{d\theta} = \frac{p}{2\pi} \frac{2\pi r^2}{p C_{cyl}} \quad (36)$$

$$= \frac{r^2}{C_{cyl}} \quad (37)$$

$$C_{cyl} = r^2 C_{jnt} \triangleq T_C(C_{jnt}) \quad (38)$$

3.3.3 3 link mechanism

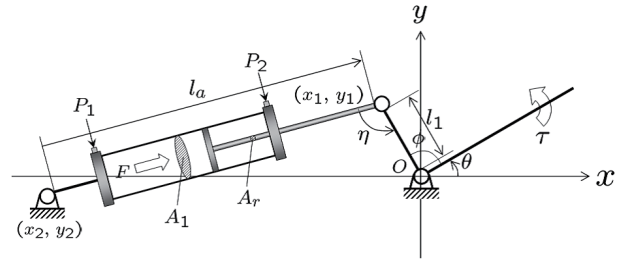


Fig. 7 .

From Fig.7, next equations are obtained geometrically.

$$x_1 = l_1 \cos(\theta + \phi), \quad (39)$$

$$y_1 = l_1 \sin(\theta + \phi) \quad (40)$$

Therefore, T_p is

$$l_a = \sqrt{(x_1 - x_2)^2 + (y_1 - y_2)^2} \quad (41)$$

$$= \sqrt{\{l_1 \cos(\theta + \phi) - x_2\}^2 + \{l_1 \sin(\theta + \phi) - y_2\}^2} \quad (42)$$

$$\triangleq T_p(\theta) \quad (43)$$

From derivation of T_p, T_v is

$$\begin{aligned} \frac{dl_a}{dt} &= \frac{1}{2\sqrt{(x_1 - x_2)^2 + (y_1 - y_2)^2}} \\ &\left\{ 2(x_1 - x_2)\frac{dx_1}{dt} + 2(y_1 - y_2)\frac{dy_1}{dt} \right\} \end{aligned} \quad (44)$$

$$\triangleq T_v \left(\theta, \frac{d\theta}{dt} \right) \quad (45)$$

Also, from Fig. 6, T_f is

$$\begin{aligned} T_f(P_1, P_2, \tau, \theta) &\triangleq A_1 P_1 - A_2 P_2 - A_r P_A - \frac{1}{R(\theta)} \tau \\ &= 0 \end{aligned} \quad (46)$$

In addition, from the force relation in the cylinder, T_c is

$$\begin{aligned} C_{\text{cyl}} &= \frac{R(\theta)l_\theta(\theta)}{\frac{1}{C_{\text{jnt}}} - \frac{dR(\theta)}{d\theta} (A_1 P_1 - A_2 P_2 - A_r P_A)} \\ &\triangleq T_C(\theta, P_1, P_2, C_{\text{jnt}}) \end{aligned} \quad (47)$$

4. CONCLUSION

We propose a "Mechanical Compliance Control System" as a new pneumatic arm control system. The main feature of the proposed system is that the two desired pressure values are calculated by using two desired values –the end compliance and the end position and posture of the arm.

In this paper, it is important to have indicated the framework of the pneumatic arm control system using pneumatic cylinders. In next step, we should present the quantitative result of simulation and real evaluation.

REFERENCES

- [1] Susumu TACHI and Taisuke SAKAKI, "Impedance Controlled Master-slave Manipulation System. Part I. Basic Concept and Application to the System with a Time Delay", *Advanced Robotics*, Vol.6, No.4, pp.483-503, 1992
- [2] Kiyoshi HOSHINO and Ichiro KAWABUCHI, "Mechanism of Humanoid Robot Arm with 7 DOFs Having Pneumatic Actuators", *IEICE Trans. on Fundamentals*, Vol. E89-A, No. 11, pp. 3290-3297, 2006
- [3] Makoto KANEKO, Kazuhito YOKOI and Kazuo TANIE, "Direct Compliance Control for Serial Link Arm: 1st Report, Basic Concept and Decoupling Condition", *Transactions of the Japan Society of Mechanical Engineers. C*, Vol. 54, No. 503, pp. 1510-1514, 1988
- [4] Toshiro NORITSUGU and Tsutomu WADA, "Control Performance and Typical Features of Pneumatic Servo System", *Journal of the Japan Hydraulics & Pneumatics Society*, Vol. 21, No. 4, pp. 417-424, 1990